Crystallization of Poly(ε-caprolactone) under Nanoparticle Confinement

by **Robert D. O'Connor**, **Qi Zhang**, **Karen L. Wooley**, and **Jacob Schaefer***

Department of Chemistry, Washington University, St. Louis, MO 63130

Dedicated to Professor *Dieter Seebach* on the occasion of his 65th birthday

Solid-state ^{13}C-NMR spectroscopy has been used to characterize the conformation of the hydrophobic poly(ε-caprolactone) core of a nanoparticle having a cross-linked hydrophilic poly(acrylic acid)/polyacrylamide shell. The amphiphilic nanoparticles were synthesized from the diblock copolymer, poly(ε-caprolactone)$_{121}$-*b*-poly(acrylic acid)$_{165}$ by self-assembly into polymer micelles, followed by cross-linking *via* condensation reactions between the carboxylic acid groups of the hydrophilic shell and the amine groups of 2,2′-(ethylenedioxy)-bis(ethylamine). NMR Experiments performed at $-30°$ on nanoparticles rapidly quenched from 60° show that the core is largely noncrystalline and locally disordered. Heating to 25° results in some crystallization, although far less than that observed for bulk poly(ε-caprolactone) homopolymer. Storage at $-30°$ results in further crystallization and conversion of most rubbery, mobile regions into more rigid, locally ordered amorphous domains. The absence of dipolar coupling between natural-abundance ^{13}C in the poly(ε-caprolactone) core of the nanoparticle, and ^{15}N labels dispersed throughout the cross-linked shell show that the interface between core and shell is sharp. The dipolar coupling measurements were accomplished by ^{13}C{^{15}N} rotational-echo double resonance.

Introduction. – Amphiphilic shell-cross-linked (SCK) nanoparticles are designed with specific compositions and dimensions of both the polymeric core and shell [1–3]. When the core is composed of crystallizeable polymer chains, and has dimensions comparable to that of the crystalline lamellar thickness, the phase-separated confining shell may affect nonequilibrium crystallization, chain melting, and recrystallization in the core [4][5]. Interruption of the core chain crystallization is expected to occur because of the restriction of lamellar growth imposed by the nanoscale confinement [6] within the cross-linked shell network, and because of the covalent connectivity that exists between the core chain segments and the wall-like shell layer. The net result should be significantly more-complicated thermal behavior for the crystalline component of an SCK, relative to that component in a linear diblock copolymer, or for the corresponding bulk homopolymer. This is the situation for an SCK made from the diblock copolymer, poly(ε-caprolactone)-*b*-poly(acrylic acid), or PCL-*b*-PAA. Macroscopic characterization of crystallization of the PCL core of the SCK by differential scanning calorimetry [7] has shown a pronounced inhibition of the formation of crystallites.

In this paper, we report the result of the microscopic characterization of the amorphous and crystalline domains of the core of a PCL-*b*-PAA derived SCK by solid-state ^{13}C-NMR spectroscopy. The local chain conformation in the core is defined by values of the isotropic ^{13}C chemical shift [8] and the local chain mobility by relaxation dynamics [9]. Core PCL chains in totally disordered amorphous domains are ^{13}C-shift resolved from chains in either crystalline or locally ordered amorphous domains, and

have motionally reduced $^{13}C,^{1}H$ dipolar coupling. In addition, the nature of the core-shell interface of the SCK (the boundary of the nanoparticle PCL core confinement) is established by measurement of the dipolar coupling between natural-abundance ^{13}C in the core and ^{15}N labels dispersed throughout the cross-linked shell.

Experimental Background and Procedures. – Rotational-echo double-resonance (REDOR) spectroscopy was used to restore the dipolar coupling between $^{13}C,^{15}N$ pairs of spins that is removed by magic-angle spinning [10]. REDOR Experiments are always done in two parts, once with rotor-synchronized dephasing pulses (S) and once without (S_0). The dephasing pulses change the sign of the heteronuclear dipolar coupling, and this interferes with the spatial averaging resulting from the motion of the rotor. The difference in signal intensity ($\Delta S = S_0 - S$) for the observed spin in the two parts of the REDOR experiment is directly related to the corresponding distance to the dephasing spin [11]. REDOR spectroscopy has found application in the characterization of binding sites of proteins [12–14], and in the analysis of heterogeneous biological materials such as amyloid plaques [15], membrane-protein helical bundles [16][17], insect cuticle [18], bacterial cell walls [19], and spider silk [20]. REDOR spectroscopy has also been used recently to characterize chain packing in glassy polymers [21].

REDOR NMR Experiments were performed with a 4-frequency transmission-line probe [22] having a 14-mm long, 9-mm inside-diameter anal. coil, and a *Chemagnetics/Varian* stator and spinner housing. Quenched and annealed samples were contained in *Chemagnetics/Varian* 7.5-mm outside-diameter Zr rotors. The rotors were spun at 5000 Hz with the speed under active control to within ±2 Hz. Experiments were done with a 7.05-Tesla magnet (300 MHz for ^{1}H) and a *Chemagnetics* spectrometer console. Radiofrequency pulses were produced by *American Microwave Technology* power amplifiers. The π-pulse lengths were 6.3 μs for ^{15}N and 10 μs for ^{13}C. Standard *XY-8* phase cycling [23] was used for all dephasing pulses. $^{1}H,^{13}C$ Cross-polarization transfers in CPMAS experiments were achieved in 2 ms at 50 kHz. Proton dipolar decoupling was 88 kHz during data acquisition. FTMAS NMR Spectra were acquired (with the same spectrometer) as a two rotor-cycle *Hahn* echo following a single ^{13}C $\pi/2$ inspection pulse and ^{1}H decoupling at 88 kHz.

Results and Discussion. – *Nanoscale Confinement of Crystalline Polymer Chain Segments.* The confinement of the PCL chain segments was facilitated by the assembly of amphiphilic block copolymers, PCL_{121}-*b*-PAA_{165}, into polymer micelles in aqueous solution, followed by covalent cross-linking between the PAA residues *via* amidation reactions. This general methodology locks-in the limited PCL domain size, and, even upon collection of the materials in the bulk, the nanoscale structure is maintained. Therefore, growth of PCL crystallites is restricted to the volume adopted during the formation of the supramolecular polymer micelles. A simplified structure for the SCKs produced for this study is illustrated in *Fig. 1*. On a mica surface, SCKs containing a PCL core have a height of *ca.* 10 nm and a diameter that is 5–10 times larger, as measured by atomic-force microscopy [24][25]. This disk-shaped geometry suggests a lamellar crystalline phase. Yet, differential scanning calorimetry has revealed that the SCK-entrapped PCL chains achieve only a fraction of the percentage of crystallinity exhibited by PCL or PCL-*b*-PAA [24]. Solid-state NMR experiments were, therefore, conducted because of their unique ability to characterize the amorphous, nanoconfined PCL chains.

Line Assignments. The CPMAS ^{13}C-NMR spectrum of PCL_{121}-*b*-PAA_{165} SCK quenched from 60° to liquid-N_2 temperature (with data acquisition at −30°) is shown in *Fig. 2* (bottom). The five narrower lines are assigned to the PCL core. The C=O C-atom peak of PCL is at 172 ppm, with the amide C=O C-atom resonance of the PAA shell appearing as a low-field shoulder. Sufficient ^{15}N-labeled cross-linker was added so that about half of the PAA carboxylic acids have been converted to amides [26]. The C=O C-atom peak for the remaining carboxylic acids appears under the PCL 172-ppm

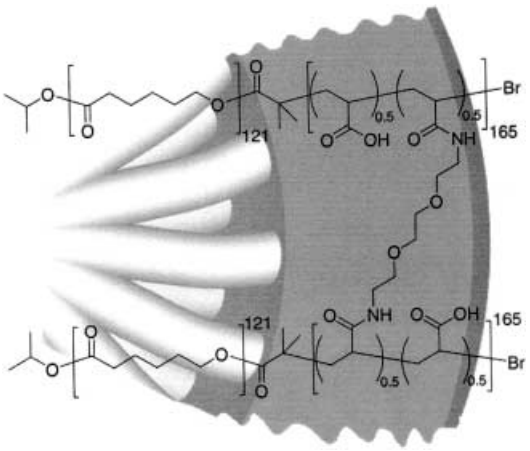

Fig. 1. *A structural formula and schematic drawing for an SCK*. The structural formula represents an idealized composition, containing a stoichiometry of *ca.* 1:1 acid/amide functionalities, but neglects illustration of the intramolecular looping and mono-attachment reactions that can occur between the poly(acrylic acid) residues and the diamino cross-linker. The schematic drawing shows a portion of the SCK shell in gray and the core chains as white cylinders.

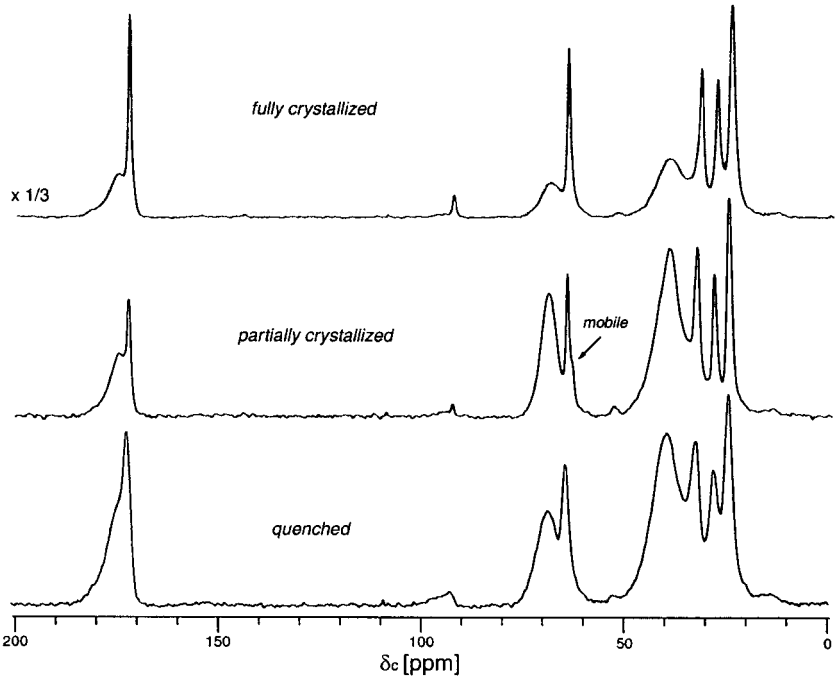

Fig. 2. *CPMAS ^{13}C NMR Spectra of poly(ε-caprolactone)$_{121}$-b-poly(acrylic acid)$_{165}$* nanoparticles, shell cross-linked by 2,2′-(ethylenedioxy)bis(ethyl[^{15}N]amine), which have been quenched in liquid N_2 and then heated to $-30°$ (*bottom*), partially crystallized by room-temperature annealing (*middle*), and more completely crystallized by storage for 2 d at $-30°$ (*top*). The spectra have been scaled (× 1/3; top; × 1; middle and bottom) for equal peak heights at 40 ppm.

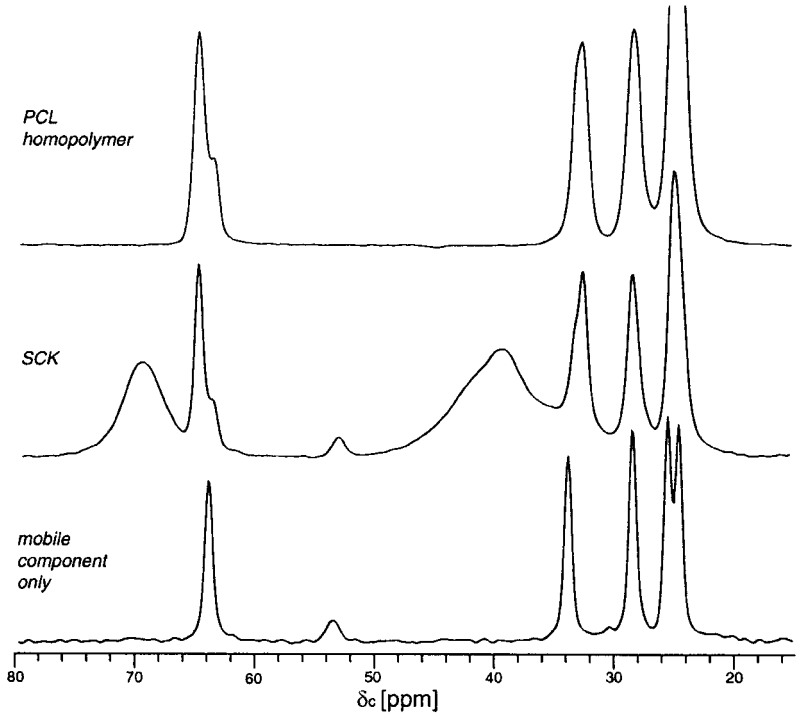

Fig. 3. *FTMAS* (bottom) *and CPMAS* (middle) *^{13}C-NMR spectra of the partially crystallized nanoparticle of* Fig. 1. The region of the spectra between 20 and 80 ppm is shown. The recycle time of the FTMAS experiment was 1 s. Only those C-atoms with short ^{13}C spin-lattice relaxation times are observed. A part of the CPMAS ^{13}C-NMR spectrum of bulk poly(ε-caprolactone) homopolymer is shown at the top of the figure.

peak. The highest-field PCL line is double intensity and arises from the two innermost CH_2 C-atoms of the repeating unit. The CH and CH_2 C-atom resonances of PAA are at 40 ppm, and the oxygenated-C-atom resonances of the crosslinker at 70 ppm.

Crystallization. After warming the quenched sample of *Fig. 2* (bottom) to 25°, all of the PCL lines sharpen (*Fig. 2*, middle), consistent with the formation of some crystalline regions in the core. In addition, the oxygenated CH_2 C-atom PCL peak at 64 ppm has developed a noticeable high-field shoulder. This shoulder is assigned to conformational kinks or defects that are part of PCL rubber. Similar shifts are observed in the spectrum of bulk PCL homopolymer (*Fig. 3*, top). The rubbery regions of the SCK core have a short ^{13}C spin-lattice relaxation time and are the only components visible in a FTMAS spectrum obtained with a short recycle time (*Fig. 3*, bottom).

The relative intensities of the 64-ppm peak and its shoulder for bulk PCL homopolymer differ from those of PCL in the SCK core (*Fig. 3*, middle). This difference means that the nanoconfinement that the shell places on the PCL core has affected crystallization in the core (the degree of crystallinity is less by a factor of 2 as measured by thermal analysis; see [7]), as well as the distribution of chains into crystalline and amorphous domains. This control is exerted globally because there is no observed interpenetration of PCL and PAA chains at the interface. ^{13}C{^{15}N} REDOR

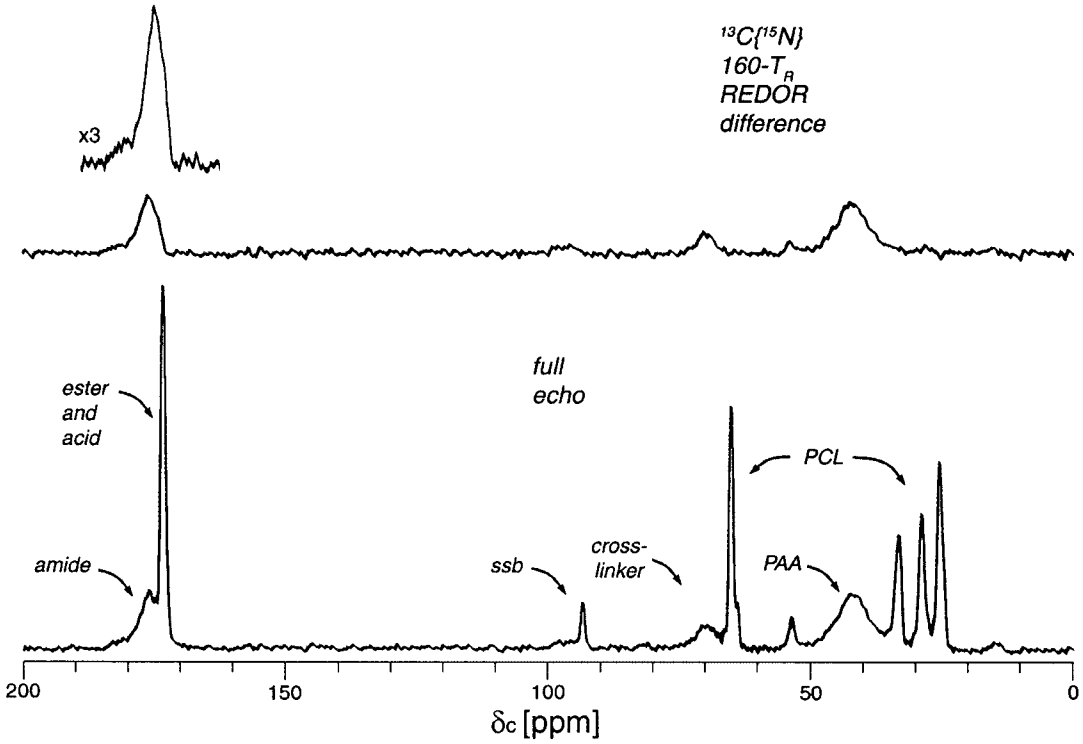

Fig. 4. *$^{13}C\{^{15}N\}$ REDOR Dephasing* ($\Delta S/S_0$) *for the partially crystallized nanoparticle of* Fig. 1. The REDOR differences after 160 rotor cycles of dipolar evolution are shown at the top of the figure, and the full echoes at the bottom. All of the REDOR difference signals are associated with carbons in the shell. Magic-angle spinning was at 5 kHz.

Spectra (*Fig. 4*) show no dipolar contact between PCL natural-abundance ^{13}C in the core, and ^{15}N labels in the shell ($^{13}C-^{15}N$ distance separations greater than 6 Å). This is true even though some of the ^{15}N cross-linking labels have been detected at the core-shell interface in similar SCKs made from poly(*p*-fluorostyrene)-*b*-poly(acrylic acid) [27].

Structure of the Core. Following storage of the SCK of *Fig. 2* (middle) at $T = -30°$ for 2 d, the intensities of the five PCL lines all increase (*Fig. 2*, top). The crystallinity of PCL core also increases but still does not match the levels observed for bulk homopolymer [7]. The relative intensities of the core ester (PCL) and shell acid and amide (PAA/polyacrylamide) C=O C-atom peaks are now close to the stoichiometric ratio of 121:165. This means that highly mobile amorphous regions, which are difficult to cross-polarize and, so, are poor contributors to the CPMAS spectrum [9], have largely been eliminated. Because the crystallinity of the SCK core is still low [7], the increase in signal intensity must arise from relatively rigid amorphous regions that are easily cross-polarized. Consistent with this notion, the disappearance of the shoulder on the 64-ppm peak (*Fig. 2*, middle) indicates that many defect conformations have been eliminated. Thus, compared to bulk PCL homopolymer, the PCL core of the SCK

nanoparticle consists of fewer crystalline domains and fewer major-defect (kinked) conformations, but more locally ordered chains in amorphous regions within which chains have only minor packing variations [21].

This work was supported by *NSF* grant DMR-9974457 (*K. L. W.*) and *NSF* grant DMR-0097202 (*J. S.*).

REFERENCES

[1] K. B. Thurmond II, T. Kowalewski, K. L. Wooley, *J. Am. Chem. Soc.* **1996**, *118*, 7239.
[2] V. Bütün, N. C. Billingham, S. P. Armes, *J. Am. Chem. Soc.* **1998**, *120*, 12135.
[3] Q. Zhang, E. E. Remsen, K. L. Wooley, *J. Am. Chem. Soc.* **2000**, *122*, 3642.
[4] L. Zhu, S. Z. D. Cheng, B. H. Calhoun, Q. Ge, R. P. Quirk, E. L. Thomas, B. S. Hsiao, F. Yeh, B. Lotz, *J. Am. Chem. Soc.* **2000**, *122*, 5957.
[5] S. Nojima, K. Hashizume, A. Rohadi, S. Sasaki, *Polymer* **1997**, *38*, 2711.
[6] Y.-L. Loo, R. A. Register, A. J. Ryan, G. T. Dee, *Macromolecules* **2001**, *34*, 8968.
[7] Q. Zhang, C. G. Clark Jr., E. E. Remsen, T. Kowalewski, K. L. Wooley, submitted for publication.
[8] A. C. de Dios, J. G. Pearson, E. Oldfield, *Science* **1993**, *260*, 1491.
[9] V. J. McBrierty, K. J. Packer, 'Nuclear Magnetic Resonance in Solid Polymers', Cambridge University Press, Cambridge, 1993.
[10] T. Gullion, J. Schaefer, *J. Magn. Reson.* **1989**, *81*, 196.
[11] T. Gullion, J. Schaefer, *Adv. Magn. Reson.* **1989**, *13*, 58.
[12] D. R. Studelska, C. A. Klug, D. D. Beusen, L. M. McDowell, J. Schaefer, *J. Am. Chem. Soc.* **1996**, *118*, 5476.
[13] L. M. McDowell, A. Schmidt, E. R. Cohen, D. A. Studelska, J. Schaefer, *J. Mol. Biol.* **1996**, *256*, 160.
[14] Y. Li, B. Poliks, L. Cegelski, M. Poliks, Z. Gryczynski, G. Piszcek, P. G. Jagtap, D. R. Studelska, D. G. I. Kingston, J. Schaefer, S. Bane, *Biochemistry* **2000**, *39*, 281.
[15] J. J. Balbach, Y. Ishii, O. N. Antzutkin, R. D. Leapman, N. W. Rizzo, F. Dyda, J. Reed, R. Tycko, *Biochemistry* **2000**, *39*, 13748.
[16] S. O. Smith, T. Kawakami, W. Liu, M. Ziliox, S. Aimoto, *J. Mol. Biol.* **2001**, *313*, 1139.
[17] J. Wang, Y. S. Balazs, L. K. Thompson, *Biochemistry* **1997**, *36*, 1699.
[18] M. E. Merritt, A. M. Christensen, K. J. Kramer, T. L. Hopkins, J. Schaefer, *J. Am. Chem. Soc.* **1996**, *118*, 11278.
[19] G. Tong, Y. Pan, H. Dong, R. Pryor, G. E. Wilson, J. Schaefer, *Biochemistry* **1997**, *36*, 9859.
[20] C. A. Michal, L. W. Jelinski, *J. Biomol. NMR* **1998**, *12*, 231.
[21] R. D. O'Connor, B. Poliks, D. H. Bolton, J. M. Goetz, J. A. Byers, K. L. Wooley, J. Schaefer, *Macromolecules* **2002**, *35*, 2608.
[22] J. Schaefer, R. M. McKay, U. S. Patent 5,861,748, 1999.
[23] T. Gullion, D. B. Baker, M. S. Conradi, *J. Magn. Reson.* **1990**, *89*, 479.
[24] Q. Zhang, C. G. Clark Jr., M. Wang, E. Remsen, K. L. Wooley, *Nano Lett.*, in press.
[25] Q. Zhang, E. E. Remsen, K. L. Wooley, *J. Am. Chem. Soc.* **2000**, *122*, 3642.
[26] H. Huang, K. L. Wooley, J. Schaefer, *Macromolecules* **2001**, *34*, 547.
[27] H.-M. Kao, R. D. O'Connor, A. K. Mehta, H. Huang, B. Polisk, K. L. Wooley, J. Schaefer, *Macromolecules* **2001**, *34*, 544.

Received May 29, 2002